17

Optimal Circular Flight of Multiple UAVs for Target Tracking in Urban Areas[1]

Jongrae Kim[1] and Yoonsoo Kim[2]
[1]*Department of Aerospace Engineering, University of Glasgow*
[2] *Department of Mechanical and Mechatronic Engineering, University of Stellenbosch*
[1]*U.K.*, [2]*South Africa*

1. Abstract

This work is an extension of our previous result in which a novel single-target tracking algorithm for fixed-wing UAVs (Unmanned Air Vehicles) was proposed. Our previous algorithm firstly finds the centre of a circular flight path, r_c, over the interested ground target which maximises the total chance of keeping the target inside the camera field of view of UAVs, J, while the UAVs fly along the circular path. All the UAVs keep their maximum allowed altitude and fly along the same circle centred at r_c with the possible minimum turn radius of UAVs. As discussed in [1,4], these circular flights are highly recommended for various target tracking applications especially in urban areas, as for each UAV the maximum altitude flight ensures the maximum visibility and the minimum radius turn keeps the minimum distance to the target at the maximum altitude.

Assuming a known probability distribution for the target location, one can quantify J, which is incurred by the travel of a single UAV along an arbitrary circle, using line-of-sight vectors. From this observation, (the centre of) an optimal circle $\mathcal{C}^*$ among numerous feasible ones can be obtained by a gradient-based search combined with random sampling, as suggested in [1]. This optimal circle $\mathcal{C}^*$ is then used by the other UAVs jointly tracking the same target. As the introduction of multiple UAVs may minimise J further, the optimal spacing between the UAVs can be naturally considered. In [1], a typical line search method is suggested for this optimal spacing problem. However, as one can easily expect, the computational complexity of this search method may undesirably increase as the number of UAVs increases.

The present work suggests a remedy for this seemingly complex optimal spacing problem. Instead of depending on time-consuming search techniques, we develop the following algorithm, which is computationally much more efficient. Firstly, We calculate the distribution $J(x)$, where x is an element of $\mathcal{C}^*$, which is the chance of capturing the target by one camera along $\mathcal{C}^*$. Secondly, based on the distribution function, $J(x)$, find separation angles between UAVs such that the target can be always tracked by at least one UAV with a guaranteed probabilistic measure. Here, the guaranteed probabilistic measure is chosen by taking into account practical constraints, e.g. required tracking accuracy and UAVs'

[1] This work has been supported by Subcommittee B in the University of Stellenbosch, South Africa

minimum and maximum speeds. Our proposed spacing scheme and its guaranteed performance are demonstrated via numerical simulations.
Key words: target tracking; optimal circular flight; multiple UAVs

2. Introduction and Problem Statement

Motivated by our previous novel formulation for the STTP (Single-Target Tracking Problem) using multiple UAVs (Unmanned Air Vehicles) in [1], we extend our previous ideas of handling the STTP using multiple UAVs in this work. The STTP to be considered here can be stated as follows:

Problem 2.1 *Given a ground-based target and fixed-wing UAVs equipped with a camera, find an optimal strategy in a known urban environment such that the target is kept inside at least one camera's field-of-view.*

Due to the importance and enormous applications of this problem, it has attracted a great deal of attention from researchers and has been studied in various directions, e.g. target identification or classification, fault-tolerant target tracking, multi-sensor target tracking, target position estimation. See [1] for a detailed literature review. However, it is our observation that most of the existing works are mainly focused on sensory data processing or fusion. In this work, we are more interested in *path planning* for target trackers, especially in densely populated urban domains. As far as our knowledge is concerned, there are very few works in this research area. We note that [2,3] directly address the present STTP. In particular, [3] poses the STTP as a stochastic optimisation and then proposes a real-time genetic algorithm which gradually improves an initially guessed solution.

In this present work, we develop a deterministic algorithm which is computationally much more efficient than the existing algorithms. As suggested in [1, 4], the main idea here begins with using circular motions of the fixed-wing UAVs tracking the same target. These UAVs' circular motions are highly recommended for various target tracking applications especially in urban areas, as for each UAV the maximum altitude ensures the maximum visibility and the minimum radius turn keeps the minimum distance to the target at the maximum altitude. More precisely, we first find a position, r_c, over the interested target (location), r_{tar}, which maximises the total chance of keeping the target inside the camera field of view, J, during the circular motions of the UAVs around r_c. Here, all the UAVs tracking r_{tar} keep their maximum allowed altitude $\bar{h}_{uav}$ and fly along the same circle C^*, centred at r_c with the UAVs' minimum turn radius $\underline{r}_{uav}$. We assume that the probability distribution $p(t)$ of the target location at time t is known. Note that, as the UAVs are a fixed-wing type in our present discussion, the following practical constraints are part of the STTP:

$$0 < \underline{\omega} \leq \omega_i \leq \overline{\omega} \quad \text{for} \quad i = 1, 2, \ldots, n, \tag{1}$$

where ω_i is the turning rate (magnitude) of the ith UAV, and $\underline{\omega}$ and $\overline{\omega}$ are the minimum and the maximum turning rates of UAVs, respectively. In contrast with [1], we here use ω_i as a control variable to solve the STTP problem. Note that the minimum radius turn is a function of angular velocity and bank angle. Therefore, in order to turn with the minimum radius but different speed, the angular speed must be increased or decreased by thrust, and bank angle must be adjusted appropriately so that the minimum turn radius can be maintained.

In §3.1, we first summarise how to find r_c and $\mathcal{C}^*$. For more details, we direct readers to the reference [1]. Once the UAVs' flying path $\mathcal{C}^*$ is determined, it is natural to question about how to place more than one UAV on $\mathcal{C}^*$. To answer this question, our present work is focused on the following problem:

Problem 2.2 *Determine spacing Φ between the UAVs flying along $\mathcal{C}^*$ such that at least one UAV keeps the target inside its camera's field-of-view all the time.*

This UAV spacing problem is mathematically formulated in §3.2 and two spacing schemes are proposed thereafter. Finally, numerical examples will demonstrate the efficacy of the proposed spacing schemes in §4.

3. UAV Path Planning for STTP

3.1 Optimal circle over target

In this section, we briefly summarise a method to find the centre r_c of an optimal circular path, along which UAVs fly and track a target at r_{tar}.[2]

Suppose t_c is the current time and the optimal circular path is updated every t_{com} seconds. Then, assuming a known probability density function $p(r_{tar})$ of the target location during the time interval $[t_c, t_c + t_{com}]$ (or at $t_c + t_{com}/2$), one can quantify J incurred by any UAV's travel (360-degree turn) along a circular path $\mathcal{C}$ using line-of-sight vectors, i.e.

$$J(\mathcal{C}) = \int_{x\in\mathcal{C}} \left[\int_{y\in\mathcal{S}(x)} p(y)\, dy \right] dx, \tag{2}$$

where $\mathcal{S}(x)$ is the set of all the ground locations within the UAV's camera's field-of-view at $x \in \mathcal{C}$. Thus, the following optimisation problem is of our interest:

$$\mathcal{C}^* = \underset{\mathcal{C}}{\operatorname{argmax}}\ J(\mathcal{C}).$$

A sub-optimal $\mathcal{C}^*$ (centred at r_c with a radius of $\underline{r}_{uav}$) may be obtained by a gradient-based search (starting with a circle whose centre is precisely over the most probable target location) combined with a random sampling scheme. Note that this search is not much computationally involved as long as a moderate number of samples is used to approximate the integration (2).

3.2 Spacing Strategy I

Once $\mathcal{C}^*$ is calculated, we allow more UAVs to join $\mathcal{C}^*$ for tracking the same target. As the introduction of more UAVs on $\mathcal{C}^*$ may decrease the chance of losing the target further, we are now interested in finding spacing between the UAVs so that the target is always within at least one UAV's camera's field-of-view.

Suppose the first UAV is placed on $\mathcal{C}^*$ at $x_1 = r_c + [\underline{r}_{uav}\cos\theta_1, \underline{r}_{uav}\sin\theta_1]$[3] and other $n-1$ UAVs are placed on $\mathcal{C}^*$ according to the following sequence of spacing,

$$\Phi = \{\Phi_1, \Phi_2, \ldots, \Phi_{n-1}\},$$

[2] See [1] for more details.

[3] The z coordinate of x_1 is the maximum altitude that the first UAV can assume, and is dropped in the expressions hereafter.

where Φ_i defines the angle measured from the *i*th UAV to the (*i*+l)th UAV counterclockwise with respect to r_c. That is, $\Phi_i = \theta_{i+1} - \theta_i$ for i = 1, 2, . . . , $n-1$ and $\Phi_n = \theta_1 - \theta_n$. We then consider the following new cost function J(x), where $\mathbf{x} = [x_1, x_2, \ldots, x_n] \subset \mathcal{C}^*$,

$$J(\mathbf{x}) = \max_{i \in \{1,2,\ldots,n\}} \int_{y \in \mathcal{S}_i(x_i)} p(y)\, dy, \tag{3}$$

where $\mathcal{S}_i(x_i)$ is the set of all the ground locations within the *i*th UAV's camera's field-of-view at x_i. As x can be written in terms of angles, we also call (3) $J(\Theta)$, where $\Theta = \{\theta_1, \theta_2, \ldots, \theta_n\}$ and

$$x_i = r_c + [\underline{r}_{uav} \cos\theta_i, \underline{r}_{uav} \sin\theta_i].$$

for i = 1, 2, . . . ,n.

As implied before, the direct optimisation to find Θ may be computationally involved as the number of UAVs on $\mathcal{C}^*$ increases. For this reason, we here slightly modify the problem statement as follows:

Problem 3.1 *Find* Θ *such that the target is kept inside at least one UAV's camera's field-of-view with a fixed probability or probabilistic measure* μ*, i.e.*

$$J(\Theta) \geq \mu > 0 \tag{4}$$

as UAVs fly along $\mathcal{C}^*$.

To this end, we first consider $J(\Theta)$ when n = 1, i.e $\Theta = \theta_1 \stackrel{\text{def}}{=} \theta$. For a fixed probability distribution for the target location $p(r_{tar})$ during the time interval [t_c, t_c + t_{com}], one can compute $J(\theta)$ for each $\theta \in [0, 2\pi]$ or $x_1 \stackrel{\text{def}}{=} x \in \mathcal{C}^*$. Figure 1 depicts one period of a typical $J(\theta)$. Note that, as shown in Figure 1, $\theta_{\tau j}$, which belong to $[0, 2\pi)$ for $j = 1, 2, \ldots, n_\tau$, are the angles for which the sign of $J(\theta) - \mu$ changes. The corresponding positions to $\theta_{\tau j}$ are called *transition points*.[4]

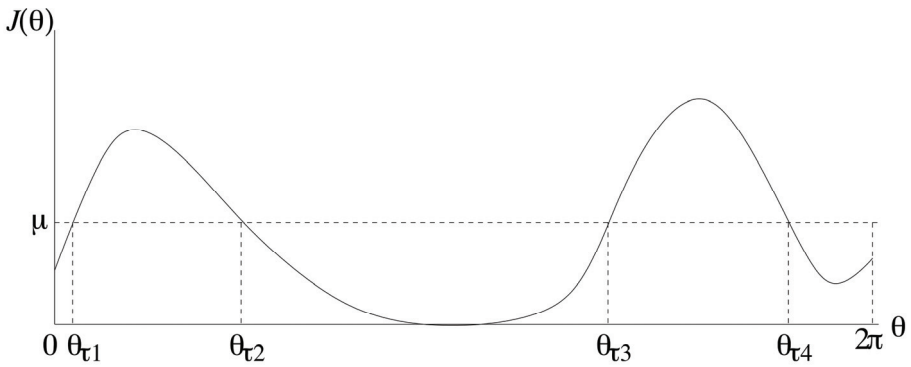

Figure 1. A typical example of $J(\theta)$ for $\theta \in [0, 2\pi]$

[4] We assume that $n_\tau \geq 1$. If $n_\tau = 0$, i.e. no transition point exists, (4) is trivially satisfied.

Our first spacing strategy is given in Table 1.[5] Clearly, this strategy guarantees the existence of at least one UAV flying along a *positive section* of $\mathcal{C}^*$ in which $J(\theta) \geq \mu$. Indeed, it guarantees an even better bound on average.

(1)	Place the ith UAV at $x_i = r_c + [\underline{r}_{uav}\cos\theta_{\tau k}, \underline{r}_{uav}\sin\theta_{\tau k}]$, where $k = \mathtt{mod}(i, n_\tau)$. That is, $k = i$ if n is less than or equal to n_τ; otherwise, ith-UAV, where $i > n_\tau$, is placed at one of the already occupied transition points.
(2)	UAV's angular speeds are chosen such that the times to travel between any two consecutive transition points are all equal. UAVs keep constant angular speeds during their flights between two consecutive transition points.

Table 1. Spacing Strategy I

Theorem 3.1 *Spacing Strategy I given in Table 1 guarantees (4). Furthermore, during UAVs' 360-degree turns along $\mathcal{C}^*$,*

$$J(\Theta) \geq \mu + \frac{2}{n_\tau|\overline{\mathcal{I}^+}|}\int_{\theta\in\mathcal{I}^+}[J(\theta)-\mu]\,d\theta, \tag{5}$$

on average, where $\mathcal{I}^+$ is the set of intervals in which $J(\theta) \geq \mu$, and $|\overline{\mathcal{I}^+}|$ is the length of the largest interval in $\mathcal{I}^+$.

Proof: As $J(\Theta) > \mu$ is straightforward to prove, we prove the second part only. Suppose

$$\mathcal{I}^+ = \{[\theta_{\tau 1}, \theta_{\tau 2}], [\theta_{\tau 3}, \theta_{\tau 4}], \ldots\} \tag{6}$$

and the interval lengths in $\mathcal{I}^+$ are l_1, l_3, . . ., respectively. In view of the second part of Spacing Strategy I, we set T to the time to travel between any two consecutive transition points. Then, for the example profile of $J(\theta) = J(\theta_1)$ as shown in Figure 2, if two UAVs start at $\theta_{\tau 1}$ and $\theta_{\tau 2}$ at $t = 0$ and turn 360 degrees along the circle, the corresponding $J(\Theta)$ in the time-domain can be calculated as shown in Figure 3. As seen in the figures, each positive part (peak) of $J(\theta)-\mu$ in the θ-domain appears twice with its stretched, shrunk or modified shape in the time-domain, depending on the two UAVs' locations.

More precisely, when t belongs to the interval $[(k-1)T, kT)$ for some $k = 1, 2, \ldots, n_\tau$, the cost is given by

$$J(\Theta) = \mu + \max_{i\in\{1,2,\ldots,n\}}[J(\theta_i)-\mu] = \mu + \max_{i\in\{1,2,\ldots,n\}}[J(\theta_{0k}+\omega_{ik}t)-\mu],$$

where ω_{ik} is the constant angular velocity of the ith UAV during the given time interval, and for $i = 1,2, \ldots, n$

$$\begin{aligned}\theta_i &= \frac{\theta_{\tau k}(t_{ik}+T) - \theta_{\tau(k+1)}t_{ik}}{T} + \omega_{ik}t \\ &= k\theta_{\tau k} - (k-1)\theta_{\tau(k+1)} + \omega_{ik}t \stackrel{\text{def}}{=} \theta_{0k} + \omega_{ik}t,\end{aligned}$$

where t_{ik} is the time when the ith UAV is at θ_{ik}.

[5] We here do not consider collision avoidance issues between UAVs.

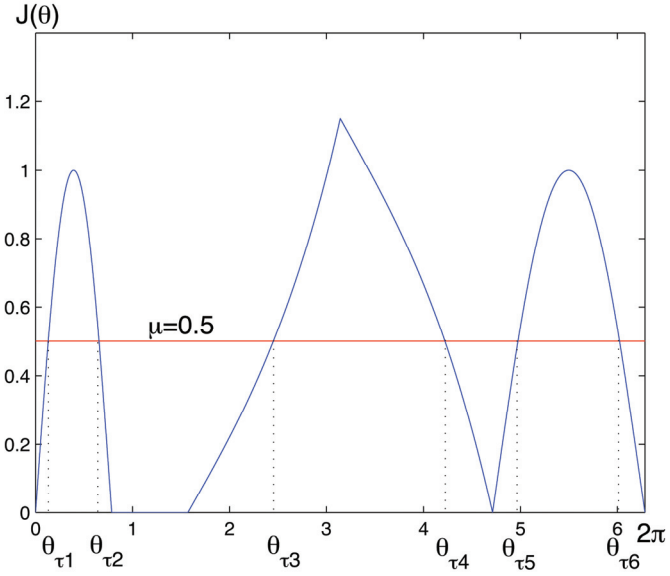

Figure 2. An example profile of $J(\theta)$ for $\theta \in [0, 2\pi]$; $\theta_{\tau j}$ (j = 1,2,..., 6) are transition points

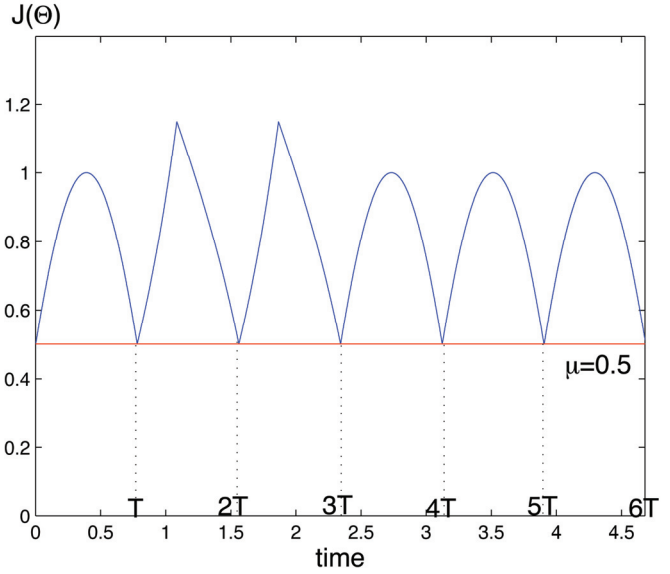

Figure 3. $J(\Theta)$ for the $J(\theta)$ shown in Figure 2: T is the time for UAVs to travel between any two consecutive transition points

Therefore, the mean value of $J(\theta)$ during UAVs' 360-degree turns can be expressed as

$$\mu + \frac{1}{n_\tau T}\sum_{k=1}^{n_\tau}\int_{(k-1)T}^{kT}\left\{\max_{i\in\{1,2,\ldots,n\}}[J(\theta_{0k}+\omega_{ik}t)-\mu]\right\}dt$$
$$\geq \mu + \frac{2}{n_\tau T}\sum_{k=1}^{n_\tau/2}\int_{2(k-1)T}^{(2k-1)T}[J(\theta_{0k}+\omega_{1k}t)-\mu]\,dt.$$

Note that n_τ is always an even number when $J(\theta)$ is continuous. Using the constant angular velocity assumption between any two consecutive transition points, one can easily check that for each k = 1, 2, . . . , $n_\tau/2$,

$$\frac{1}{T}\int_{2(k-1)T}^{(2k-1)T}[J(\theta_{0k}+\omega_{1k}t)-\mu]\,dt = \frac{1}{l_{2k-1}}\int_{\theta_{\tau(2k-1)}}^{\theta_{\tau(2k)}}[J(\theta_1)-\mu]\,d\theta_1$$
$$\geq \frac{1}{|\overline{\mathcal{I}}^+|}\int_{\theta_{\tau(2k-1)}}^{\theta_{\tau(2k)}}[J(\theta_1)-\mu]\,d\theta_1.$$

Thus, the claimed inequality follows. ■

This theorem allows us to approximately calculate average $J(\Theta)$ (guaranteed average *performance level)* once $\mathcal{C}^*$ is given, regardless of the time T to travel between any two consecutive transition points. It is obvious that one may wish to choose μ, so that the performance level in (2.5) becomes as high as possible, but this may result in transition points between which the interval is too small. Clearly, such a small interval makes UAVs flight infeasible. Therefore, μ must be determined based on various flight constraints such as (1). In the next section, we modify the first spacing strategy to accommodate those flight constraints.

3.3 Spacing Strategy II

In this section, we take into account flight constraints on UAV's travel speed and time along $\mathcal{C}^*$. In view of (1.1), μ must be chosen such that

$$\underline{\omega}T \leq l_i \leq \overline{\omega}T \quad \forall i,$$

where $l_i = \theta_{\tau(i+1)} - \theta_{\tau i}$, as defined in (6).

These flight constraints immediately imply that μ cannot be arbitrarily large. In this regard, we propose the second spacing strategy which now involves a search for a proper μ. The second strategy starts with setting μ to the average $J(\theta)$ over $0 \leq \theta \leq 2\pi$, i.e. $\int_0^{2\pi} J(\theta)\,d\theta/2\pi$, and check if there exist(s) an interval(s) $[\chi_{2j-1}, \chi_{2j}]$ $(j = 1, 2, \ldots, n_\chi) \subset \mathcal{I}_i^+$ in (6) such that

$$\begin{aligned}
&\underline{\omega}T \leq \chi_{2j} - \chi_{2j-1} \leq \overline{\omega}T \quad \forall j = 1, 2, \ldots, n_\chi,\\
&\underline{\omega}T \leq \frac{\chi_{2j+1} - \chi_{2j}}{n-1} \leq \overline{\omega}T \quad \forall j = 1, 2, \ldots, n_\chi - 1 \text{ (if } n_\chi > 1),\\
&\underline{\omega}T \leq \frac{2\pi - (\chi_{2n_\chi} - \chi_1)}{n-1} \leq \overline{\omega}T,
\end{aligned} \tag{7}$$

are satisfied. If there exist such intervals, one can increase μ and repeat the same step above. Otherwise, one should decrease μ until such intervals are found and the search is terminated.

Once the search is finished with a proper μ and its corresponding $[\chi_{2j-1}, \chi_{2j}]$, UAVs are placed on $\mathcal{C}^*$ at

$$x_1 = r_c + [\underline{r}_{uav} \cos \chi_1, \underline{r}_{uav} \sin \chi_1] \tag{8}$$

and if $n_\chi > 1$,

$$\begin{aligned} x_i = r_c \quad + \quad & \left\{ \underline{r}_{uav} \cos \left[\chi_2 + \frac{i-2}{n-1}(\chi_3 - \chi_2) \right], \right. \\ & \left. \underline{r}_{uav} \sin \left[\chi_2 + \frac{i-2}{n-1}(\chi_3 - \chi_2) \right] \right\}, \end{aligned} \tag{9}$$

otherwise

$$\begin{aligned} x_i = r_c \quad + \quad & \left\{ \underline{r}_{uav} \cos \left[\chi_2 + \frac{i-2}{n-1}(2\pi + \chi_1 - \chi_2) \right], \right. \\ & \left. \underline{r}_{uav} \sin \left[\chi_2 + \frac{i-2}{n-1}(2\pi + \chi_1 - \chi_2) \right] \right\} \end{aligned} \tag{10}$$

for i = 2,3, . . . ,n.

The conditions in (7) ensure that at least one UAV flies over one of the intervals in $\mathcal{I}^+$, and so $J(\theta) \geq \mu$. In fact, one can easily show that the bound obtained in Proposition 2.1 still holds.

(1) Maximise μ subject to (7).
(2) Place UAVs at the locations specified by (8), (9) and (10).

Table 2. Spacing Strategy II

Theorem 3.2 *Spacing Strategy II guarantees (4) and (5).*

However, finding such intervals may not be a simple task, as $\mathcal{I}^+$ is likely to be non-convex (a union of disjoint intervals). In this regard, assuming that there is a small number of intervals in $\mathcal{I}^+$, one can go through every possible combination of intervals in J^+ to find feasible $[\chi_{2j-1}, \chi_{2j}]$ (j = 1,...,n_χ).[6] In fact, we start the search with the case of n_χ = 1. For example, consider an interval $[\theta_{\tau 1}, \theta_{\tau 2}] \subset \mathcal{I}^+$ and solve the following linear program for χ_1, χ_2 and T: minimise T subject to

$$\begin{aligned} & \theta_{\tau 1} \leq \chi_1 \leq \theta_{\tau 2}, \quad \theta_{\tau 1} \leq \chi_2 \leq \theta_{\tau 2}, \quad \underline{\omega} T \leq \chi_2 - \chi_1 \leq \overline{\omega} T, \\ & \underline{\omega} T \leq \frac{2\pi - (\chi_2 - \chi_1)}{n-1} \leq \overline{\omega} T. \end{aligned}$$

[6] MILP (Mixed Integer Linear Programming) could be used for this purpose.

If no feasible solution is found for each interval in $\mathcal{I}^+$, n_χ is now increased to 2 and two intervals are chosen from $\mathcal{I}^+$.[7] For example, we choose $[\theta_{\tau 1}, \theta_{\tau 2}]$, $[\theta_{\tau 3}, \theta_{\tau 4}] \in \mathcal{I}_i^+$, and solve the following linear program for χ_1, χ_2, χ_3, χ_4 and T: minimise T subject to

$$\begin{aligned}
&\theta_{\tau 1} \le \chi_1 \le \theta_{\tau 2}, \quad \theta_{\tau 1} \le \chi_2 \le \theta_{\tau 2}, \quad \theta_{\tau 3} \le \chi_3 \le \theta_{\tau 4}, \quad \theta_{\tau 3} \le \chi_4 \le \theta_{\tau 4}, \\
&\underline{\omega} T \le \chi_2 - \chi_1 \le \overline{\omega} T, \quad \underline{\omega} T \le \chi_4 - \chi_3 \le \overline{\omega} T, \\
&\underline{\omega} T \le \frac{\chi_3 - \chi_2}{n-1} \le \overline{\omega} T, \quad \underline{\omega} T \le \frac{2\pi - (\chi_4 - \chi_1)}{n-1} \le \overline{\omega} T.
\end{aligned}$$

When this trial is still not successful with different two intervals in $\mathcal{I}^+$, n_χ is increased (up to $n_\tau/2$) and gives rise to similar linear programs as above. If no feasible solution is found for each n_χ, μ must be decreased to relax the constraints.[8]

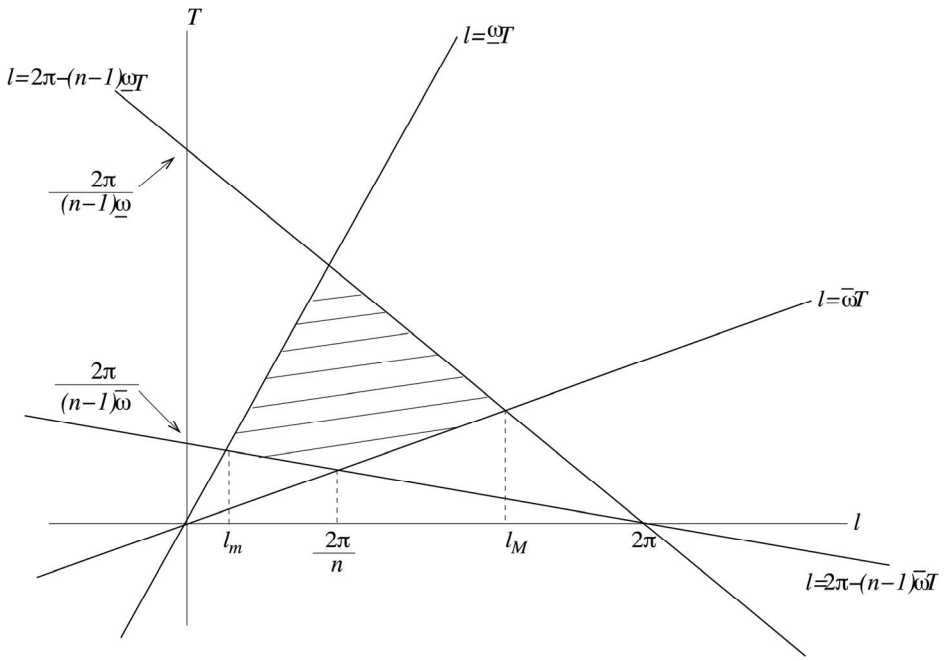

Figure 4. The polygon (dashed area) formed by the constraints when n_χ = 1

[7] When time is critical, one may not want to increase n_χ, but to decrease μ and keep considering the case of n_χ = 1 with new $\mathcal{I}^+$.

[8] It is not exactly true that less μ implies less stringent constraints. However, it is true that decreasing μ eventually yields a feasible solution.

As a matter of fact, the case of n_χ = 1 allows a more efficient way of obtaining the solution. First note that the constraints in the associated linear program can be written as

$$\underline{\omega}T \le l \le \overline{\omega}T \quad \text{and} \quad \underline{\omega}T \le \frac{2\pi - l}{n-1} \le \overline{\omega}T,$$

where $l = \chi_2 - \chi_1$. These two constraints in l and T form a polygon in two-dimensional space, as shown in Figure 4. From the figure, one can read that the minimum and maximum l possible in the polygon are

$$l_m = \frac{2\pi}{1 + (n-1)(\overline{\omega}/\underline{\omega})} \quad \text{and} \quad l_M = \frac{2\pi}{1 + (n-1)(\underline{\omega}/\overline{\omega})}.$$

Therefore, in order for some μ to be feasible, the corresponding $\mathcal{I}^+$ must contain an interval whose length is in between l_m and l_M. If there exists such an interval(s) in $\mathcal{I}^+$ whose lengths are $l_1, l_2, \ldots$, one can then read the corresponding $T_1, T_2, \ldots$ from the figure, i.e.

$$T_j = \begin{cases} (2\pi - l_j)/(n\overline{\omega} - \overline{\omega}) & \text{if} \quad l_m \le l_j \le 2\pi/n, \\ l_j/\overline{\omega} & \text{if} \quad 2\pi/n < l_j \le l_M. \end{cases}$$

Thus, the solution $[\chi_1,\ \chi_2]$ is the interval in $\mathcal{I}^+$ whose length l^* is such that T_j is minimised over all j. One can repeat finding $[\chi_1,\ \chi_2]$ with an increased μ to improve the solution.

4. Numerical Tests

To demonstrate the performance of the suggested algorithm (Spacing Strategy II), we randomly generate urban-area maps and model a ground target as a random jump process. As the employed strategy directs, each UAV flies along a designed circular path (consisting of several segments which are defined by separation angle(s)) at a different speed, but at a constant speed along each segment. In our tests, UAVs' minimum turn radius is assumed to be equal to 200 m, and their flight altitude is fixed to 100 m. The corner velocity, i.e. the velocity for a minimum radius turn at a maximum rate, is 30 m/s (approximately 100 km/h). Therefore, the maximum angular rate ($\overline{\omega}$) is given by 0.15 rad/s. The minimum angular velocity ($\underline{\omega}$) is assumed to be equal to the half of the maximum rate, i.e. 0.075 rad/s. The number of UAVs is two and they are of the same type.

One test example is shown in Figure 5. In the figure, two UAVs fly along the optimised circular path (thick solid line) in a counterclockwise direction, with an initial separation of 130 degrees. The starting position of each UAV is indicated by a triangle. The ground moving target (denoted by a red star) jumps to a random place every 1 s. Note that the target's operational area is densely populated by buildings, and thus tracking the target is very challenging. The simulation shows that, as expected, the two UAVs swap their starting positions and reach there at the same time by changing their angular velocities. Figure 6 shows $J(\theta)$ (dotted line; before introducing two UAVs), $J(\Theta)$ (solid line; after introducing two UAVs with the separation angle suggested by our spacing strategy), and the corresponding lower bound μ. The actual cost slightly violates the lower bound at 27 s. This violation is caused by the discretisation of $J(\theta)$ when numerically obtaining

separation angles. A finer discretisation may alleviate this problem, but this slight violation does not make any significant physical difference in tracking the target. Figure 7 shows when the target is captured by the cameras. During one complete 360-degree turn along the circular path, the joint visibility is guaranteed during more than 69% of the total flight time. That is, the target is outside the two cameras' field-of-views for about 16s and the longest continuous time during which the target is lost is about 6 s.

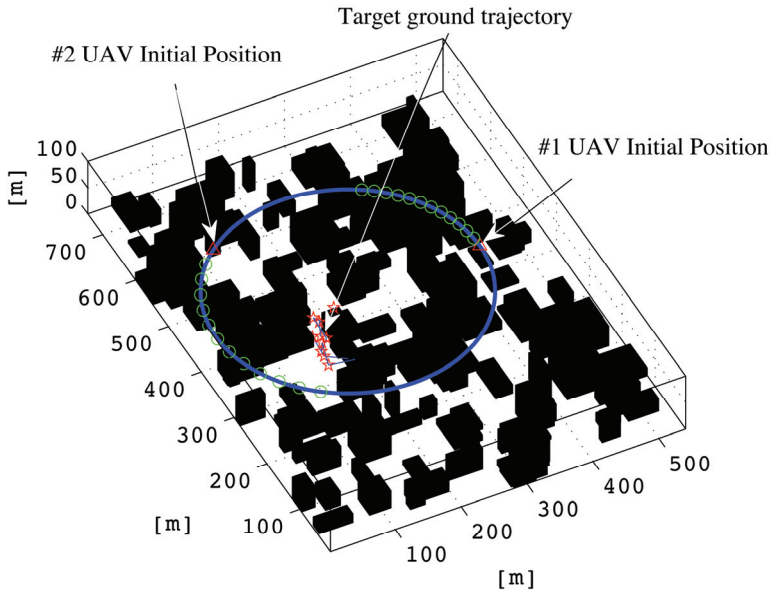

Figure 5. Two UAVs tracking a ground moving target in a dense urban area

A 1000-Monte-Carlo random simulation is also performed. This simulation is done using a personal computer (Windows-XP Professional version 2002, Intel Core 2 Quad CPU, 2.66GHz, 2.75GB of RAM, MATLAB 7.5 (R2007b)). The mean time spent to calculate separation angles for each case is 0.4963 s. In Figure 8, our proposed spacing strategy is compared with a simple separation strategy in which two UAVs are initially separated by 180 degrees. Figure 8 depicts, for both strategies, the number of cases versus the per cent of visible time during one 360-degree turn along the circular path associated with each case. The mean visibility is around 56% for both strategies. However, the variance corresponding to our spacing strategy is slightly better (smaller) than the simple one: our spacing strategy yields about 23% and the simple one about 27%. Also note that the two distributions look quite different: the distribution for the simple strategy is almost uniform, whereas the one for our proposed spacing strategy is skewed towards the right. This implies that our separation strategy handles difficult scenarios much better than the simple one.

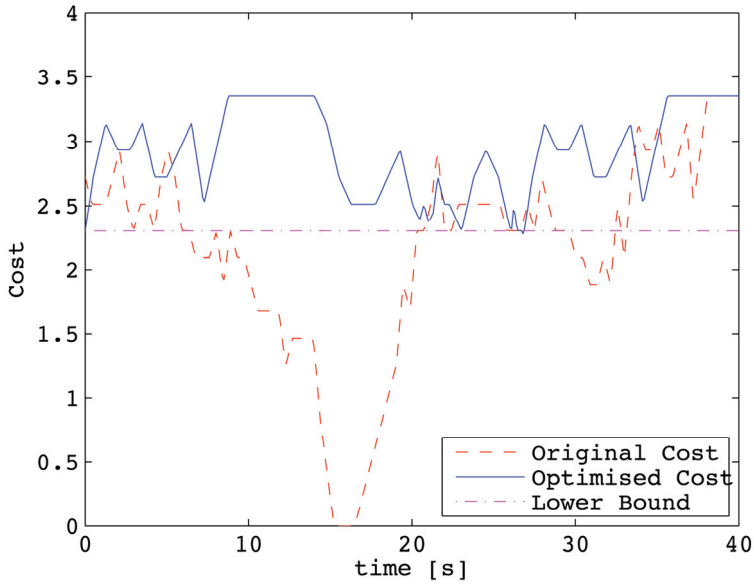

Figure 6. Original cost $J(\theta)$, optimised cost $J(\Theta)$ and lower bound

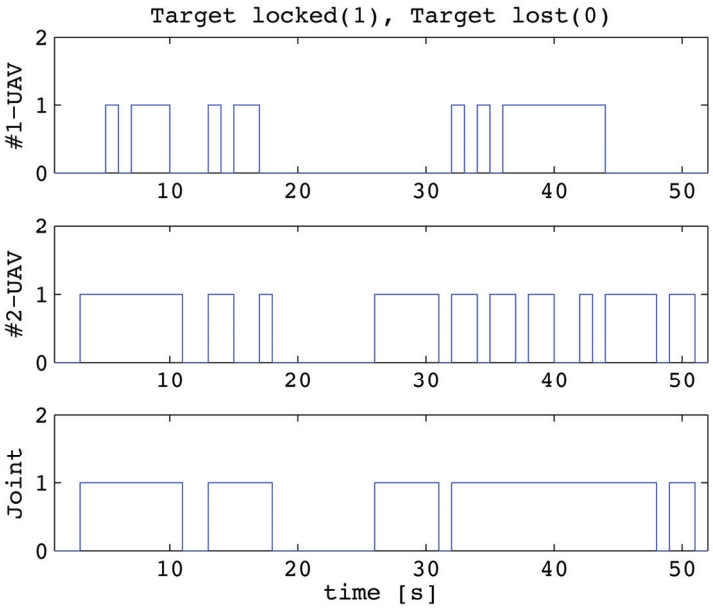

Figure 7. Target visibility during a 360-degree turn along the circular path shown in Figure 5

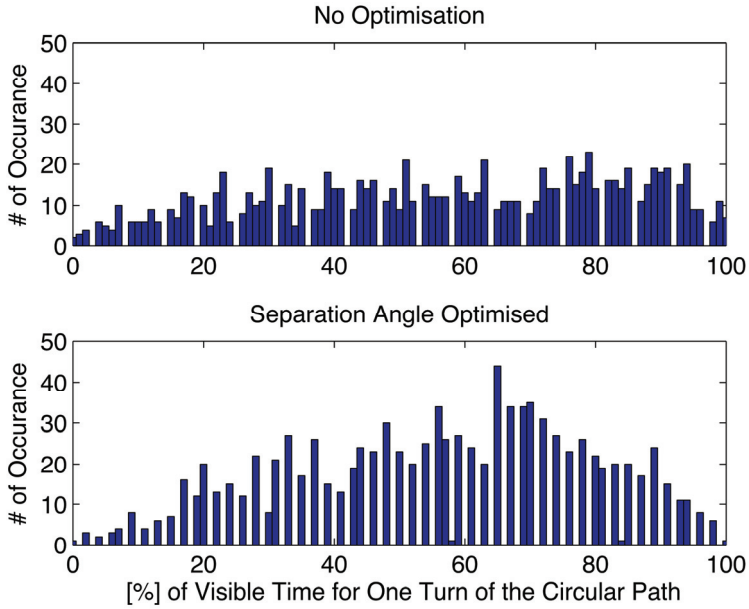

Figure 8. Target visibility distribution for 1000 random cases during a 360-degree turn along the circular path associated with each case

5. Conclusion

In this work, we extended our previous result by suggesting two spacing strategies which allow more than one UAV to jointly track a target with a guaranteed probabilistic bound. As opposed to typical line search methods, the proposed spacing strategies are independent of the number of UAVs tracking the same target in terms of computational complexity, and so easy to implement on UAVs especially with low computational power. However, there are a few points that need to be addressed in our future work. For example, suppose that a target moves beyond the area covered by a circular path $\mathcal{C}_1$, and so a new circular path $\mathcal{C}_2$ and the corresponding spacing are calculated. Then, one needs to consider a transition strategy which allows UAVs to move from $\mathcal{C}_1$ to $\mathcal{C}_2$ while still guaranteeing a probabilistic bound. Needless to say, extensions to the multiple target tracking case should be useful as well.

6. References

J. Kim and Y. Kim. Moving ground target tracking in dense obstacle areas using UAVs, In *Proceedings of the 17th IFAC World Congress,* July 2008. [1]

Mark A. Peot, Thomas W. Altshuler, Arlen Breiholz, Richard A. Bueker, Kenneth W. Fertig, Aaron T. Hawkins and Sudhakar Reddy. Planning sensing actions for UAVs in urban domains, In *Proceedings of the SPIE,* October 2005. [2]

Vitaly Shaferman and Tal Shima. Unmanned aerial vehicles cooperative tracking of moving ground target in urban environments, *Journal of Guidance, Control, and Dynamics,* Vol. 31, No. 5, September-October 2008, pp. 1360-1371. [3]

F. Rafi, S. Khan, K. Shafiq and M. Shah. Autonomous target following by unmanned aerial vehicles, In *Proceedings of the SPIE,* May 2006. [4]